Supplement of The Cryosphere, 16, 1265–1280, 2022
https://doi.org/10.5194/tc-16-1265-2022-supplement


The Cryosphere
Open Access

*Supplement of*

# Temporal variation of bacterial community and nutrients in Tibetan glacier snowpack

**Yuying Chen et al.**

*Correspondence to:* Mukan Ji (jimk@lzu.edu.cn)

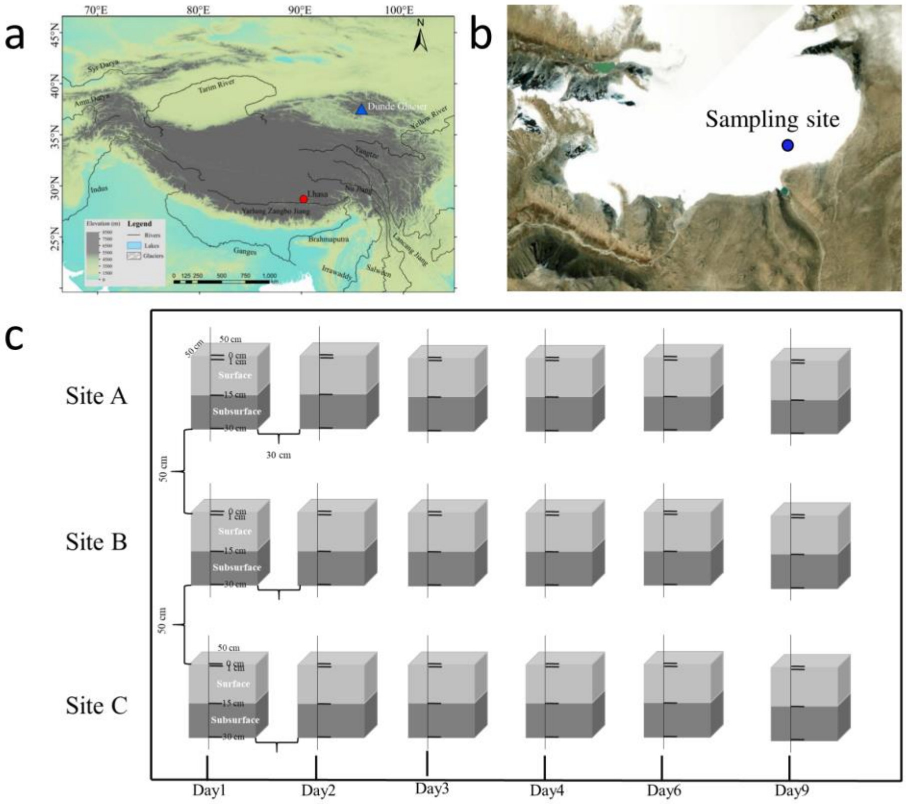


Fig. S1 Geographic location of the Dunde glacier (a and b) and schematic of sampling design.

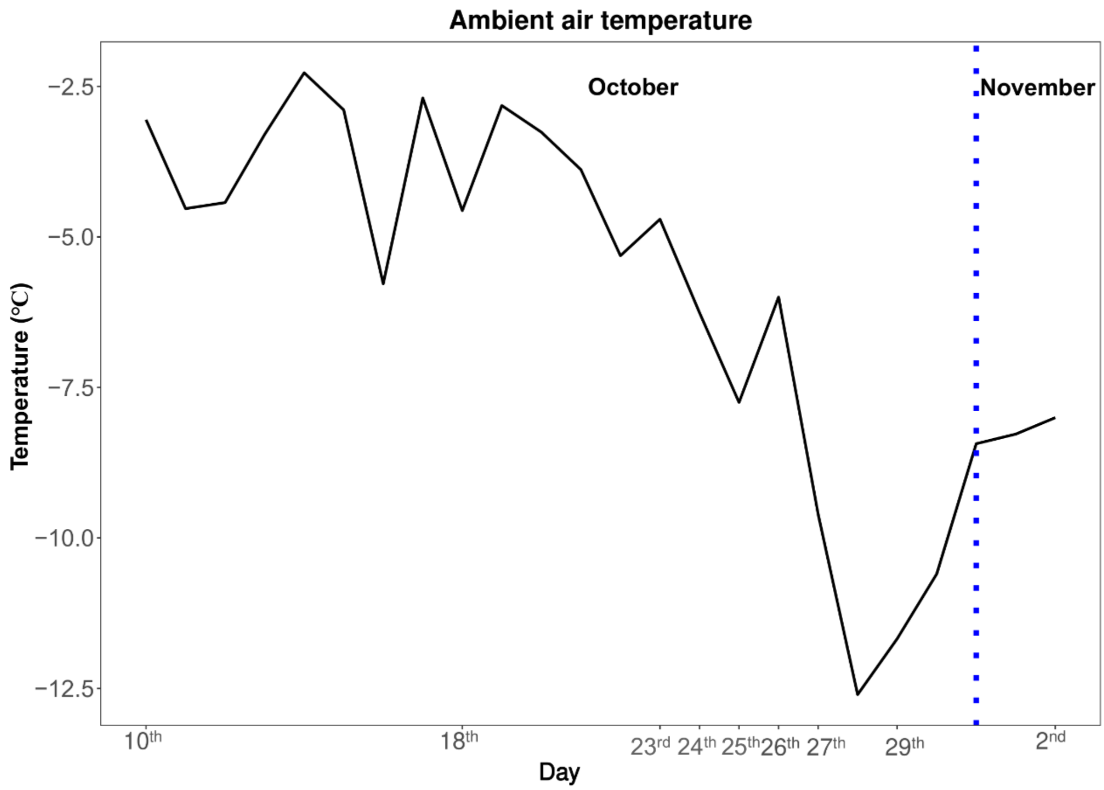


Fig. S2 Air temperature record from the first arrived the camp. Snowfall started on the [1]8th and ended on the [2]3rd of October. Sampling was conducted on the 24th, 25th, 26th, 27th, and 29th of October, and the 2nd November. The ambient air temperature during the sampling period was averaged -8 ℃.

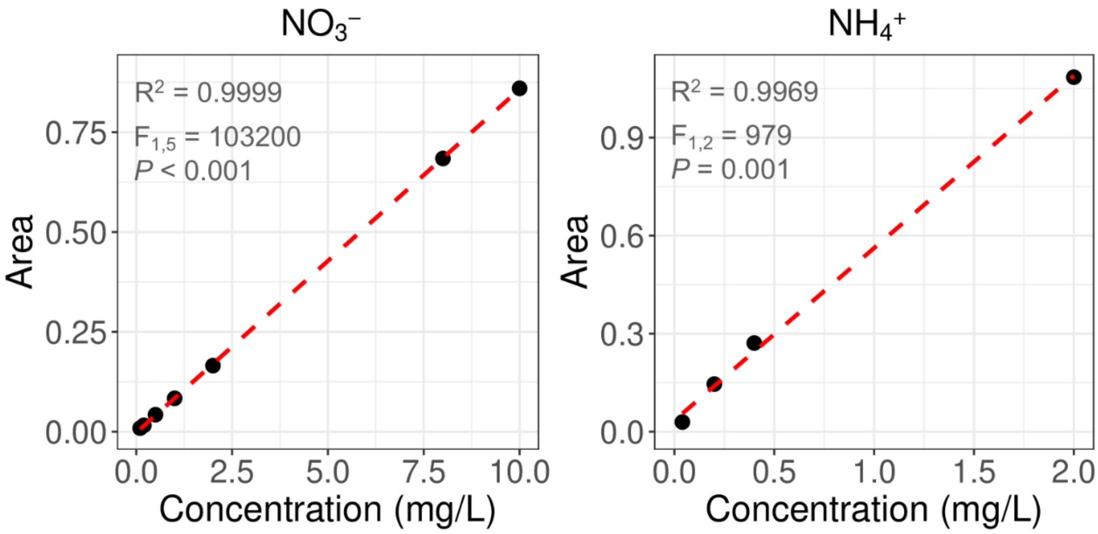


Fig. S3 Standard curve of $NO_3^-$, $NH_4^+$ ions. The x-axis is the concentration of the standard sample; the y-axis represents the peak area. Significance is based on linear regression.

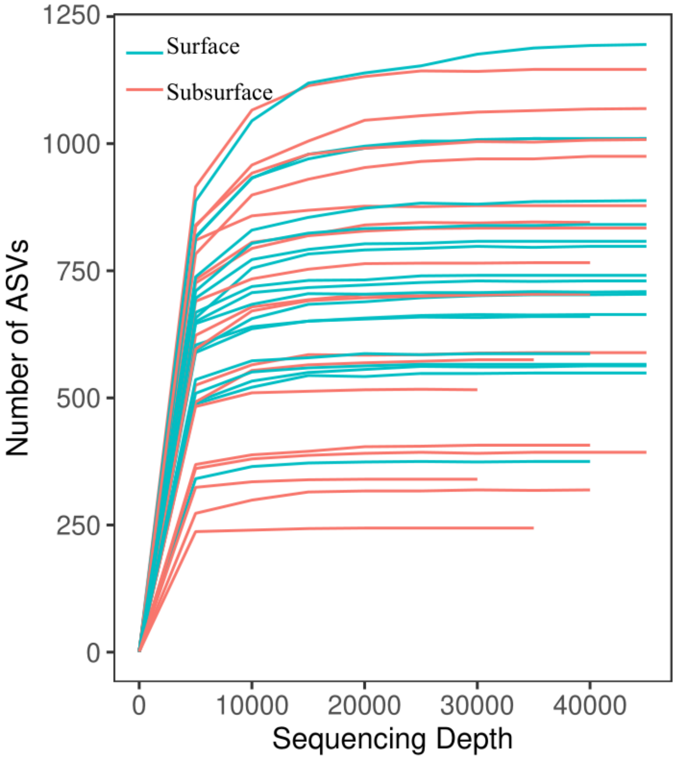


Fig. S4 Rarefaction curves for each sample, relating the number of ASVs detected as a function of the sequencing effort.

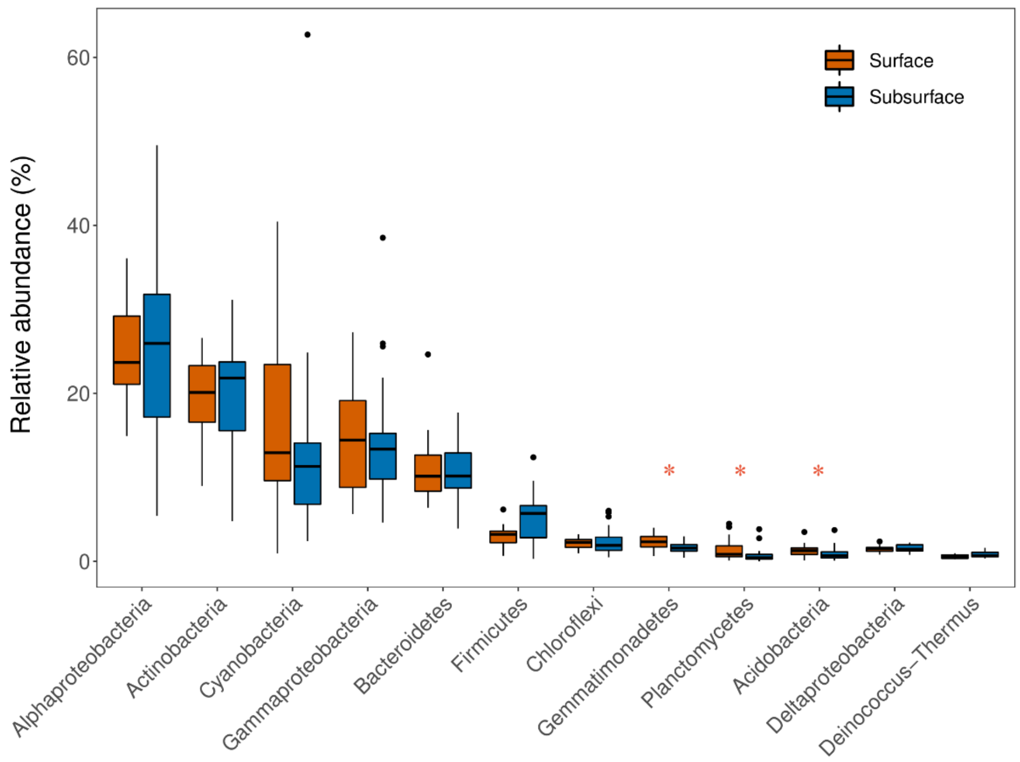


Fig. S5 Relative abundances of the dominant (average relative abundance > 1%) bacterial phyla (Proteobacteria is further classified at the class-level) in the surface and subsurface layers. Statistical significance is indicated by $^{*}P < 0.05$ based on Wilcoxon rank-sum test.

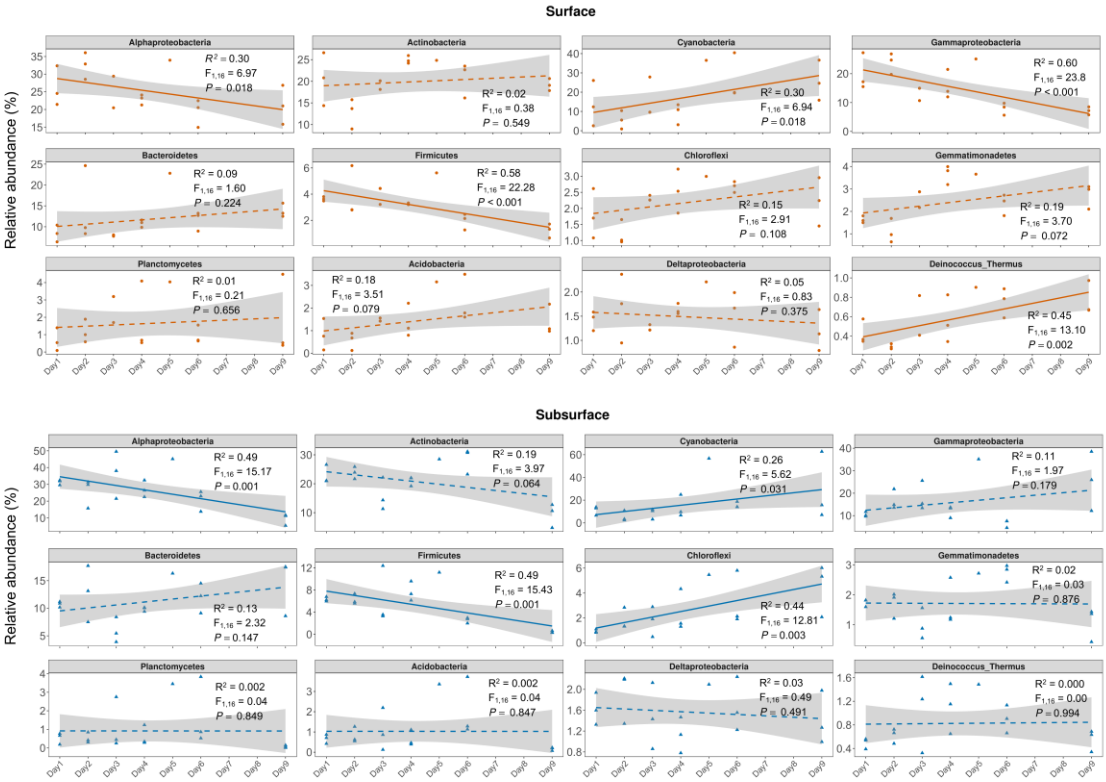

Fig. S6 Temporal changes of the relative abundance of dominant bacterial phyla in the surface and subsurface snow. Each dot represents an individual sample. The solid and dashed lines indicate significant and nonsignificant changes, respectively. Significance is based on linear regression.

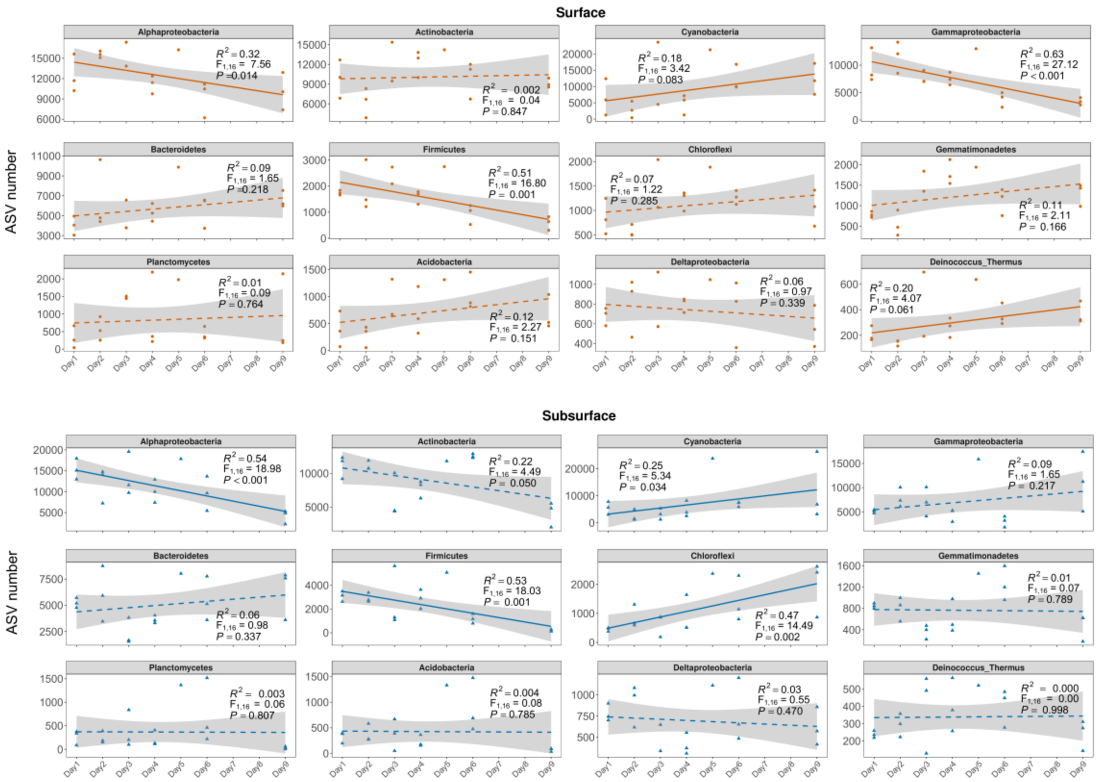


Fig. S7 Temporal changes of the ASV number of dominant bacterial phyla in the surface and subsurface snow. Each dot represents an individual sample. The solid and dashed lines indicate significant and nonsignificant changes, respectively. Significance is based on linear regression.

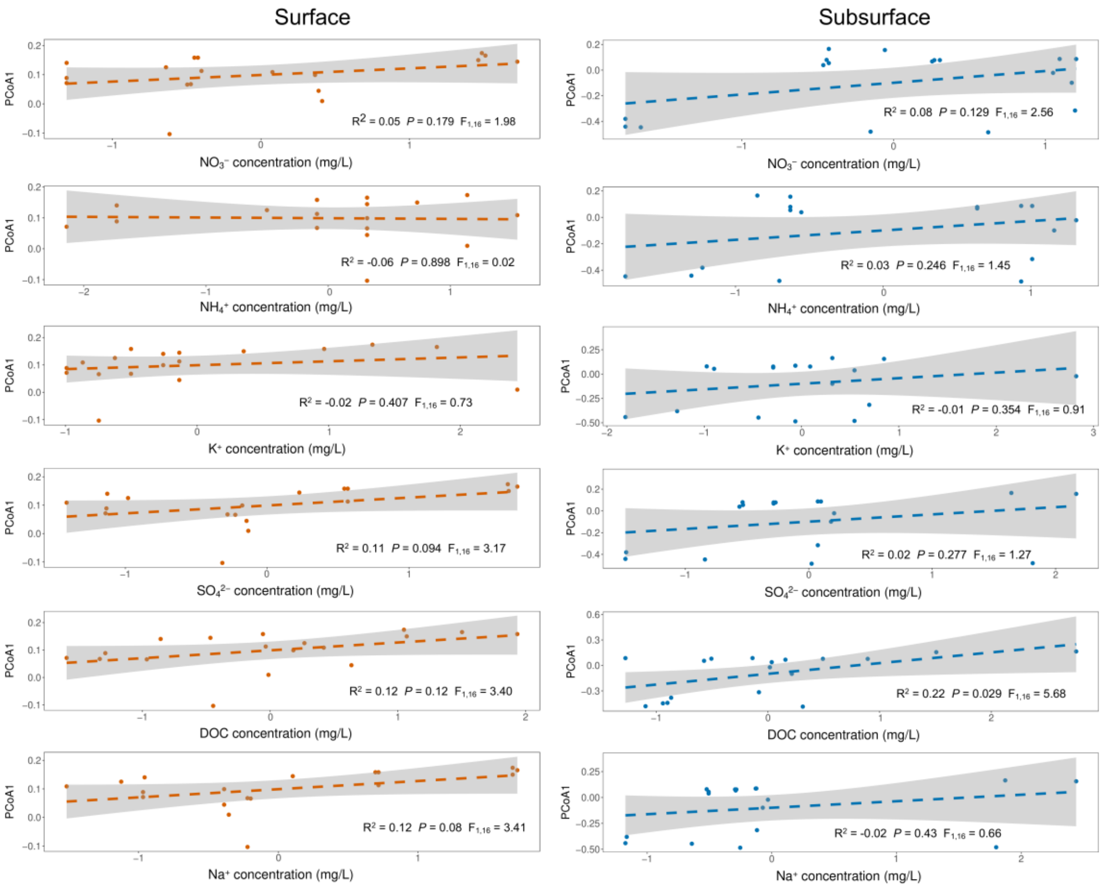


Fig. S8 Pairwise regression analyses between PCoA1 scores and environmental factors. The solid and dashed lines indicate significant and nonsignificant changes (based on linear regression at $P$ < 0.05), respectively. PCoA1 exhibits no significant relationship with the measured environmental factors in the surface snow, while in the subsurface layer, the PCoA1 is significant associated with DOC concentrations. Grey shading indicates the 95% confidence interval of regression.

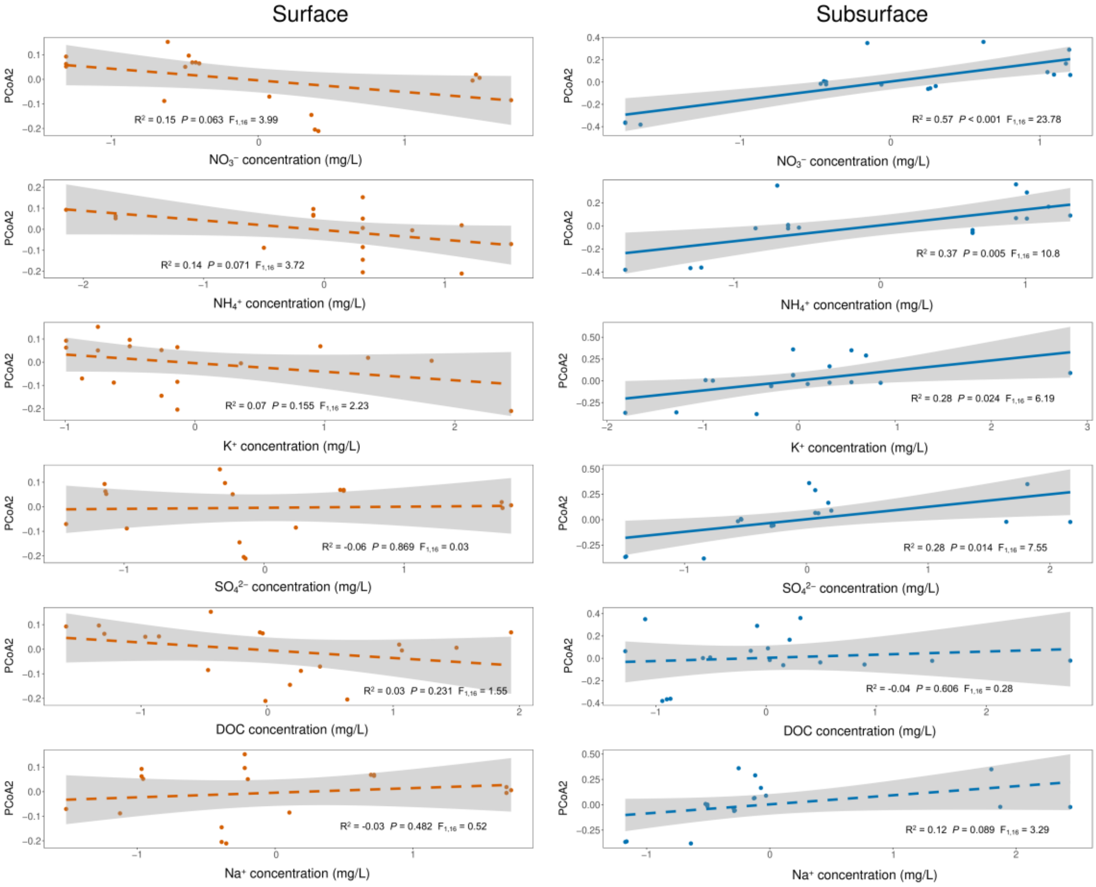


Fig. S9 Pairwise regression analyses between PCoA2 scores and environmental factors. The solid and dashed lines indicate significant and nonsignificant changes (based on linear regression at $P$ < 0.05), respectively. PCoA2 exhibits no significant relationship with the measured environmental factors in the surface layer, while in the subsurface layer, the PCoA2 is significant associated with nitrate, ammonium, potassium, sulfate, and DOC concentrations. Grey shading indicates the 95% confidence interval of regression.

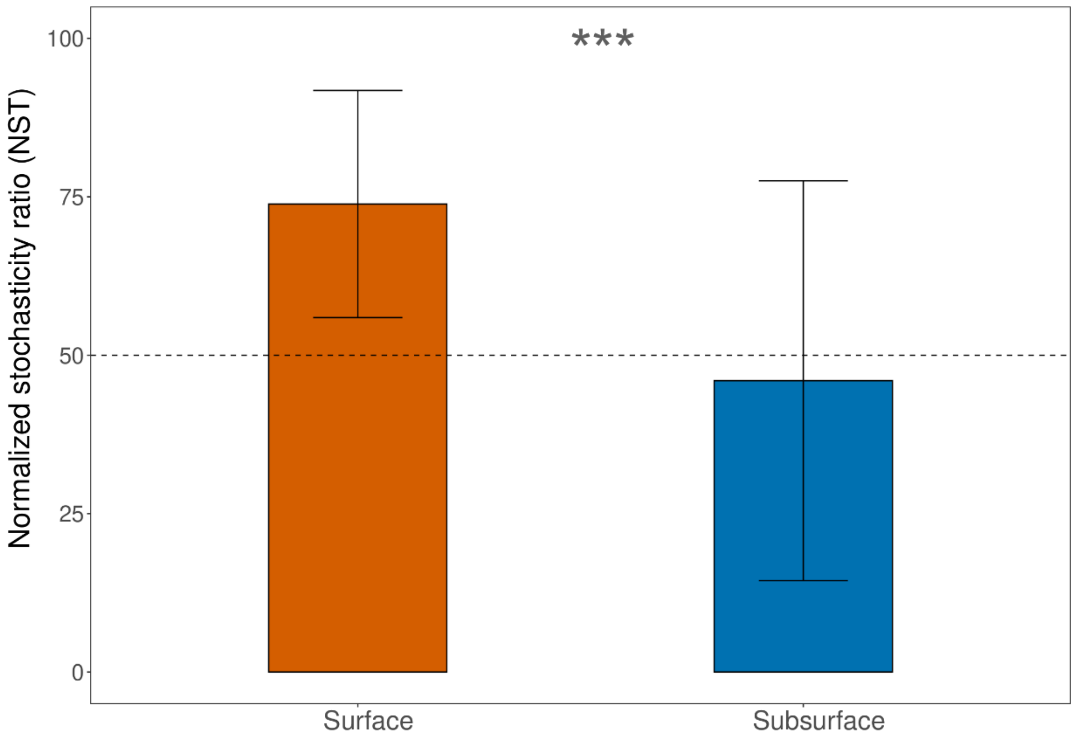


Fig. S10 Normalized stochasticity (NST) ratios estimated for the bacterial community in the surface and subsurface snow. Bar plots shows the comparison of NST between the surface and subsurface bacterial communities. *** indicates significance at $P < 0.001$. The contribution of stochasticity is significantly higher in the surface snow than that in the subsurface snow. The contribution of stochasticity was higher and lower than 50% in the surface and the subsurface layer snow, which indicates the community assembly processes are dominated by stochasticity and determinism, respectively.

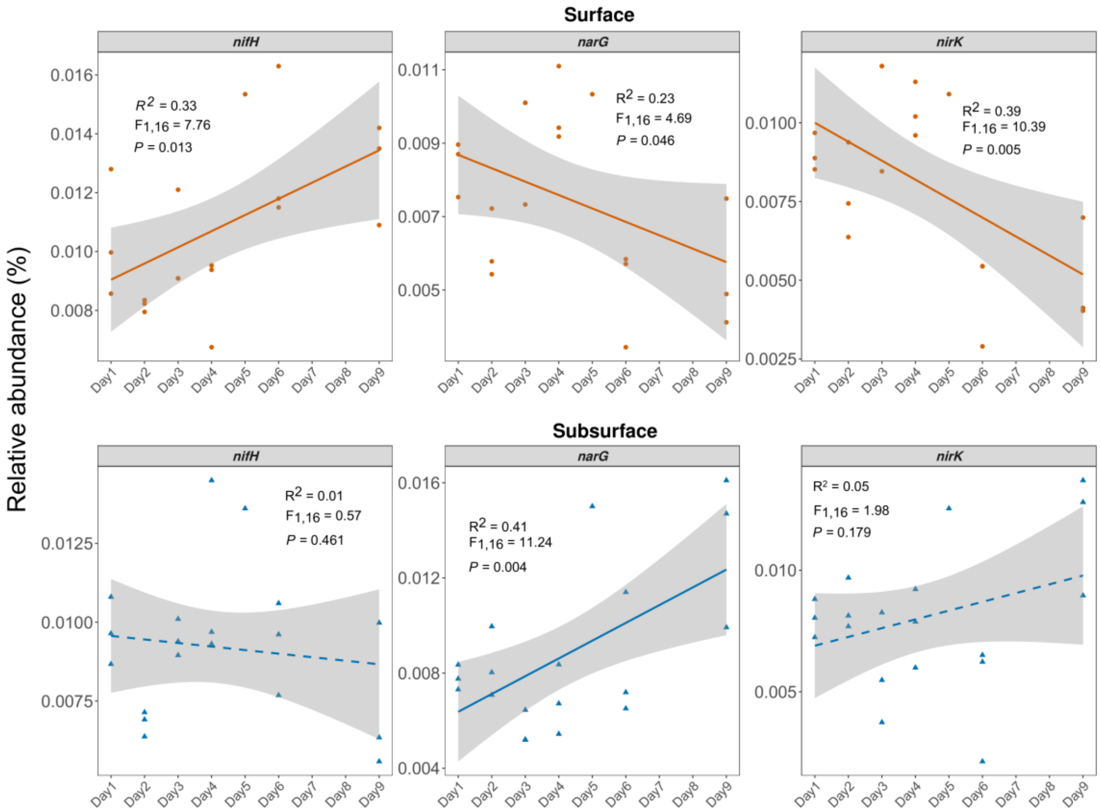


Fig. S11 The temporal changes of the relative abundance of nitrogen-cycle related genes in the surface and subsurface snow. The solid and dashed lines indicate significant and nonsignificant changes at $P < 0.05$ (based on linear regression), respectively. For the surface snow, the relative abundance of *nifH* gene significantly increases with time, while the relative abundance of *narG* and *nirK* genes significantly decreases with time. For the subsurface snow, the relative abundance of *nifH* gene is similar across the nine days, while the relative abundance of *narG* and *nirK* genes significantly and nonsignificantly increase with time, respectively. Grey shading indicates the 95% confidence interval of regression.

Table S1 physiochemical parameters of the snow samples in the surface and subsurface layer.

| Depth | Time | Sample name[a] | DOC (mg/L) | $NO_3^-$ (mg/L) [a] | $NH_4^+$ (mg/L) [a] | $K^+$ (mg/L) [a] | $SO_4^{2-}$ (mg/L) [a] | $Na^+$ (mg/L) |
|---|---|---|---|---|---|---|---|---|
| Surface | Day1 | D1.1 | 0.97 | 0.44 | 0.18 | 0.04 | 1.85 | 0.85 |
| | | D1.2 | 1.17 | 0.44 | 0.18 | 0.10 | 1.86 | 0.86 |
| | | D1.3 | 0.83 | 0.44 | 0.17 | 0.04 | 1.84 | 0.85 |
| | Day2 | D2.1 | 0.95 | 0.79 | 0.22 | 0.08 | 3.25 | 1.52 |
| | | D2.2 | 1.12 | 0.78 | 0.23 | 0.06 | 3.34 | 1.54 |
| | | D2.3 | 1.36 | 0.73 | 0.23 | 0.06 | 3.19 | 1.52 |
| | Day3 | D3.1 | 2.46 | 0.81 | 0.22 | 0.20 | 4.64 | 2.36 |
| | | D3.2 | 1.55 | 0.82 | 0.22 | 0.11 | 4.64 | 2.36 |
| | | D3.3 | 1.54 | 0.80 | 0.22 | 0.08 | 4.60 | 2.34 |
| | Day4 | D4.1 | 2.26 | 1.62 | 0.23 | 0.27 | 6.60 | 3.25 |
| | | D4.2 | 2.05 | 1.61 | 0.25 | 0.23 | 6.49 | 3.22 |
| | | D4.3 | 2.06 | 1.60 | 0.24 | 0.15 | 6.50 | 3.22 |
| | Day6 | D6.1 | 1.35 | 1.71 | 0.23 | 0.11 | 4.08 | 1.81 |
| | | D6.2 | 1.69 | 0.72 | 0.21 | 0.07 | 2.10 | 0.71 |
| | | D6.3 | 1.76 | 1.02 | 0.26 | 0.05 | 1.39 | 0.36 |
| | Day9 | D9.1 | 1.65 | 1.14 | 0.23 | 0.10 | 3.42 | 1.37 |
| | | D9.2 | 1.86 | 1.15 | 0.23 | 0.11 | 3.47 | 1.37 |
| | | D9.3 | 1.56 | 1.16 | 0.25 | 0.32 | 3.49 | 1.40 |
| Subsurface | Day1 | D1.1 | 2.21 | 3.78 | 0.53 | 0.25 | 5.18 | 2.06 |
| | | D1.2 | 2.62 | 3.85 | 0.53 | 0.30 | 5.18 | 2.05 |
| | | D1.3 | 3.11 | 3.80 | 0.53 | 0.25 | 5.23 | 2.07 |
| | Day2 | D2.1 | 1.85 | 4.94 | 0.57 | 0.28 | 6.32 | 2.38 |
| | | D2.2 | 1.92 | 5.08 | 0.58 | 0.38 | 6.32 | 2.39 |
| | | D2.3 | 0.46 | 5.09 | 0.58 | 0.28 | 6.40 | 2.37 |
| | Day3 | D3.1 | 2.28 | 5.05 | 0.60 | 0.33 | 6.66 | 2.48 |
| | | D3.2 | 2.04 | 4.88 | 0.62 | 0.66 | 6.74 | 2.56 |
| | | D3.3 | 2.40 | 4.29 | 0.57 | 0.28 | 6.16 | 2.13 |
| | Day4 | D4.1 | 1.32 | 2.84 | 0.36 | 0.17 | 4.39 | 1.64 |
| | | D4.2 | 2.06 | 2.79 | 0.37 | 0.36 | 4.30 | 1.64 |
| | | D4.3 | 1.40 | 2.82 | 0.36 | 0.16 | 4.38 | 1.61 |
| | Day6 | D6.1 | 3.86 | 3.35 | 0.36 | 0.40 | 12.98 | 7.34 |
| | | D6.2 | 5.39 | 2.84 | 0.33 | 0.33 | 11.31 | 6.24 |
| | | D6.3 | 0.68 | 3.22 | 0.35 | 0.36 | 11.86 | 6.10 |
| | Day9 | D9.1 | 0.92 | 0.99 | 0.27 | 0.05 | 1.36 | 0.35 |
| | | D9.2 | 0.87 | 1.13 | 0.21 | 0.23 | 3.41 | 1.38 |
| | | D9.3 | 0.96 | 0.99 | 0.28 | 0.12 | 1.38 | 0.37 |

[a.] The environmental parameters exhibits significant difference between the surface and subsurface snow layers.

Table S2 Results of multiple linear regression using Akaike's information criterion (AIC), correlating community alpha diversity with environmental variables. Only significant variables were displayed. Best models are in bold.

| | Diversity index | Formula | AIC | $R^2$ | *P* | Explanatory variables |
|---|---|---|---|---|---|---|
| Surface | Shannon | Shannon ~ $NO_3^-$ + $NH_4^+$ + $K^+$ + $SO_4^{2-}$ + DOC + $Na^+$ | -34.69 | 0.28 | *0.14* | $NH_4^+$ (-2.36)* |
| | | Shannon ~ $NH_4^+$ + $K^+$ + $SO_4^{2-}$ + DOC + $Na^+$ | -36.58 | 0.33 | *0.07* | $NH_4^+$ (-2.46)* |
| | | Shannon ~ $NH_4^+$ + $SO_4^{2-}$ + DOC + $Na^+$ | -37.53 | 0.35 | *0.05* | $NH_4^+$ (-2.43)* |
| | | Shannon ~ $NH_4^+$ + $SO_4^{2-}$ + DOC | -38.18 | 0.35 | *0.03* | $NH_4^+$ (-2.28)* |
| | | **Shannon ~ $NH_4^+$ + DOC** | **-38.44** | **0.33** | ***0.02*** | **DOC (3.20)**** |
| | Chao1 | Chao1 ~ $NO_3^-$ + $NH_4^+$ + $K^+$ + $SO_4^{2-}$ + DOC + $Na^+$ | 194.21 | 0.07 | *0.36* | |
| | | Chao1 ~ $NO_3^-$ + $NH_4^+$ + $K^+$ + $SO_4^{2-}$ + DOC | 192.22 | 0.15 | *0.23* | |
| | | Chao1 ~ $NO_3^-$ + $NH_4^+$ + $SO_4^{2-}$ + DOC | 190.59 | 0.20 | *0.15* | |
| | | Chao1 ~ $NO_3^-$ + $SO_4^{2-}$ + DOC | 189.54 | 0.22 | *0.1* | |
| | | **Chao1 ~ $NO_3^-$ + $SO_4^{2-}$** | **188.72** | **0.22** | ***0.06*** | **$SO_4^2$ (2,54)*** |
| Subsurface | Shannon | Shannon ~ $NO_3^-$ + $NH_4^+$ + $K^+$ + $SO_4^{2-}$ + DOC + $Na^+$ | -25.59 | 0.61 | *0.008* | $NO_3^-$ (3.79)**, $NH_4^+$ (-2.54)* |
| | | **Shannon ~ $NO_3^-$ + $NH_4^+$ + $SO_4^{2-}$ + DOC + $Na^+$** | **-26.91** | **0.63** | ***0.003*** | **$NO_3^-$ (3.98)**, $NH_4^+$ (-2.76)*, $SO_4^2$ (-2.20)*** |
| | Chao1 | Chao1 ~ $NO_3^-$ + $NH_4^+$ + $K^+$ + $SO_4^{2-}$ + DOC + $Na^+$ | 183.77 | 0.73 | *0.001* | $NO_3^-$ (5.02)***, $SO_4^{2-}$ (-4.52)***, $Na^+$ (4.34)** |

| | | | | | |
|---|---|---|---|---|---|
| | Chao1 ~ $NO_3^-$ + $NH_4^+$ + $K^+$ + $SO_4^{2-}$ + $Na^+$ | 181.77 | 0.76 | *<0.001* | $NO_3^-$ (5.25)***, $NH_4^+$ (-2.41)*, $SO_4^2$ (-5.20)***, $Na^+$ (5.22)*** |
| | **Chao1 ~ $NO_3^-$ + $NH_4^+$ + $SO_4^{2-}$ + $Na^+$** | **181.25** | **0.75** | ***<0.001*** | **$NO_3^-$ (5.40)***, $NH_4^+$ (-2,67)*, $SO_4^2$ (-5.48)***, $Na^+$ (5.40)*** ** |

* $P < 0.05$, ** $P < 0.01$, *** $P < 0.001$

Table S3 Topological properties comparison between empirical and random networks for the bacterial communities in surface and subsurface snow layers.

| | Empirical Network | | Random Network | |
|---|---|---|---|---|
| | Surface | Subsurface | Surface | Subsurface |
| Modularity | 0.65 | 0.40 | 0.43 ± 0.008 | 0.27 ± 0.029 |
| Connectedness (Con) | 0.71 | 0.86 | 0.39 ± 0.035 | 0.97 ± 0.007 |
| Transitivity (Trans) | 0.45 | 0.49 | 0.05 ± 0.010 | 0.23 ± 0.010 |
| Density (D) | 0.02 | 0.06 | 0.02 ± 0.000 | 0.06 ± 0.000 |
| Average clustering coefficient (avgCC) | 0.31 | 0.39 | 0.05 ± 0.010 | 0.18 ± 0.015 |
| Average path distance (GD) | 5.51 | 4.72 | 3.44 ± 0.055 | 2.73 ± 0.048 |